A Novel, Highly Selective Inhibitor of Pestivirus Replication That Targets the Viral RNA-Dependent RNA Polymerase

Jan Paeshuyse,[1] Pieter Leyssen,[1] Eric Mabery,[2] Nina Boddeker,[2] Robert Vrancken,[3] Matheus Froeyen,[1] Israrul H. Ansari,[4] Hélène Dutartre,[5] Jef Rozenski,[1] Laura H. V. G. Gil,[4] Carine Letellier,[3] Robert Lanford,[6] Bruno Canard,[5] Frank Koenen,[3] Pierre Kerkhofs,[3] Ruben O. Donis,[4] Piet Herdewijn,[1] Julia Watson,[2] Erik De Clercq,[1] Gerhard Puerstinger,[7] and Johan Neyts[1]*

Rega Institute for Medical Research, Katholieke Universiteit Leuven, Leuven, Belgium[1]; Gilead Sciences, Foster City, California[2]; Veterinary and Agrochemical Research Centre, Ukkel, Belgium[3]; Department of Veterinary and Biomedical Sciences, University of Nebraska—Lincoln, Lincoln, Nebraska[4]; Laboratory AFMB-UMR 6098, Marseille, France[5]; Department of Virology and Immunology, Southwest National Primate Research Center, and Southwest Foundation for Biomedical Research, San Antonio, Texas[6]; and Department of Pharmaceutical Chemistry, Institute of Pharmacy, University of Innsbruck, Austria[7]

We report on the highly potent and selective antipestivirus activity of 5-[(4-bromophenyl)methyl]-2-phenyl-5H-imidazo[4,5-c]pyridine (BPIP). The 50% effective concentration (EC_{50}) for inhibition of bovine viral diarrhea virus (BVDV)-induced cytopathic effect formation was 0.04 ± 0.01 μM. Comparable reduction of viral RNA synthesis ($EC_{50} = 0.12 \pm 0.02$ μM) and production of infectious virus ($EC_{50} = 0.074 \pm 0.003$ μM) were observed. The selectivity index (ratio of 50% cytostatic concentration/EC_{50}) of BPIP was ~2,000. BPIP was inactive against the hepatitis C virus subgenomic replicon and yellow fever virus but demonstrated weak activity against GB virus. Drug-resistant mutants were at least 300-fold less susceptible to BPIP than wild-type virus; showed cross-resistance to N-propyl-N-[2-(2H-1,2,4-triazino[5,6-b]indol-3-ylthio)ethyl]-1-propanamine (VP32947), and carried the F224S mutation in the viral RNA-dependent RNA polymerase (RdRp). When the F224S mutation was introduced into an infectious clone, the drug-resistant phenotype was obtained. BPIP did not inhibit the in vitro activity of recombinant BVDV RdRp, but did inhibit the activity of replication complexes (RCs). Computational docking revealed that F224 is located at the top of the finger domain of the polymerase. Docking of BPIP in the crystal structure of the BVDV RdRp revealed aromatic ring stacking, some hydrophobic contacts, and a hydrogen bond. Since two structurally unrelated compounds, i.e., BPIP and VP32947, target the same region of the BVDV RdRp, this position may be expected to be critical in the functioning of the polymerase or assembly of the RC. The potential of BPIP for the treatment of pestivirus and hepacivirus infections is discussed.

Pestiviruses cause important diseases of livestock such as bovine viral diarrhea in cattle, classical swine fever in pigs, and border disease in sheep. The genus *Pestivirus* is classified along with the genus *Hepacivirus* and *Flavivirus* in the family *Flaviviridae*. The members of the family display contrasting host range specificity (31). Flaviviruses multiply in arthropods and a large number of vertebrate species; pestiviruses infect cloven-hoofed animals, and hepaciviruses infect humans naturally and chimpanzees experimentally. Two biotypes of pestiviruses exist: those that result in lysis of in vitro infected cells, named cytopathogenic (CP), and those that do not, termed noncytopathogenic (NCP) (31).

Bovine viral diarrhea virus (BVDV) is a major pathogen of cattle. In the United States, most estimations of losses caused by BVDV at the national level range between $10 and $40 million per million calves (21). Losses are projected in reduced milk production, reduced reproductive performance, growth retardation, and increased mortality among young stock (21).

Also, the classical swine fever virus (CSFV) can be responsible for major economic losses, especially in countries with an industrialized pig production (14). Regardless of the availability of vaccines against BVDV and CSFV and the implementation of elaborate eradication or control programs (20, 44), both viruses remain an agronomical burden. An alternative approach to combating BVDV and CSFV infections could be the use of antiviral agents that specifically inhibit the replication of the virus. Although likely not suited to treat large herds, it may be important to have selective antipestivirus compounds on hand. For example, in case of an outbreak of CSFV, an option could be to prophylactically treat pigs that live in farms located in close proximity to the infected farm with an antipestivirus drug. Antiviral treatment may result in almost immediate protection against infection (protection following vaccination is obtained only 10 to 14 days later) and hence prevent transmission of the virus (and avoid large-scale culling of healthy animals). In the future, as pestivirus eradication programs reach their final stages, it will be important to have methods to control the spread of reintroduced viruses. Other possible uses for antipestivirus drugs could be (i) to treat valuable animals in zoologic collections, (ii) to treat expensive animals in breeding

---

* Corresponding author. Mailing address: Rega Institute for Medical Research, Minderbroedersstraat 10, B-3000 Leuven, Belgium. Phone: 32-16-337341. Fax: 32-16-337340. E-mail: johan.neyts@rega.kuleuven.ac.be.

programs and in vitro embryo production (45), and (iii) to cure established cell lines from contaminating pestiviruses (13, 19).

Recently, a number of selective anti-BVDV compounds have been reported. These include polymerase inhibitors, e.g., *N*-propyl-*N*-[2-(2*H*-1,2,4-triazino[5,6-b]indol-3-ylthio)ethyl]-1-propanamine (VP32947) (2), a thiazole urea derivative (24), a cyclic urea derivative (47), and inhibitors of the NS3/NS4A protease, for example, a boron-modified peptidyl mimetic (7). Aromatic cationic molecules were also reported to inhibit BVDV replication, although their mechanism of action remains to be elucidated (18). Other BVDV inhibitors target cellular enzymes such as α-glucosidase (4, 12, 58) and inosinate dehydrogenase (46).

BVDV is considered to be a valuable surrogate virus for hepatitis C virus (HCV) (6). HCV is a major cause of cirrhosis and primary hepatocellular carcinoma and the main reason for liver transplantations among adults in western countries (48). The current standard therapy for hepatitis C, i.e., the combination of pegylated alpha interferon and the nucleoside analogue ribavirin, is effective in only about 50 to 60% of patients who suffer from chronic HCV infection and is associated with important side effects (28). Consequently, there is an urgent need for highly effective and selective inhibitors of HCV replication.

In some aspects of viral replication, BVDV is more advantageous in comparison to the currently used HCV replicon systems (3, 17, 33, 39). The latter do not undergo a complete replication cycle; hence, early stages (attachment, entry, and uncoating) or late stages (virion assembly and release) of the viral replication cycle cannot be studied in the HCV replicon system. However, very recently, robust HCV cell culture systems have been reported (32, 51, 56). Yet, insight into the mechanism of antiviral activity of antipestivirus compounds may provide valuable information for the design of novel antiviral strategies against HCV (6).

Here, we report on the activity and mechanism of action of a novel, potent, and highly selective inhibitor of the replication of pestiviruses, 5-[(4-bromophenyl)methyl]-2-phenyl-5*H*-imidazo[4,5-c]pyridine (BPIP). Implications for the development of HCV inhibitors are discussed.

MATERIALS AND METHODS

Compounds. The synthesis of BPIP (Fig. 1) will be reported elsewhere (J. Paeshuyse, J. Neyts, P. Herdewijn, E. De Clercy, and G. Puerstinger, unpublished data). VP32947 was synthesized by standard methods. 3′-Deoxyguanosine-5′-triphosphate (3′-dGTP), 2′-*C*-methylguanosine-5′-triphosphate (2′-*C*-Me-GTP), and 2′-*O*-methylguanosine-5′triphosphate (2′-*O*-Me-GTP) were purchased from Trilink (San Diego, CA). Solubility of BPIP was determined spectrophotometrically at an optical density at 300 nm (OD$_{300}$) in minimal essential medium (MEM; Gibco, Merelbeke, Belgium) containing 5% heat-inactivated fetal bovine serum (FBS; Integro, Zaandam, The Netherlands) and in RNA-dependent RNA polymerase (RdRp) buffer (50 mM HEPES [pH 8.0], 10 mM KCl, 10 mM dithiothreitol [DTT], 1 mM MgCl$_2$, 2 mM MnCl$_2$, 0.5% igepal [Sigma, Bornem, Belgium]).

Cells and viruses. Madin-Darby bovine kidney (MDBK) cells were grown in MEM (Gibco) supplemented with 5% heat-inactivated FBS (Integro). FBS was shown to be free of BVDV type 1 (BVDV-1) and BVDV-2 by reverse transcription (RT)-PCR (30). Porcine kidney cells (PK15) were grown in MEM supplemented with 10% heat-inactivated FBS. First-passage BVDV strain NADL stock was generated from pNADLp15a as previously described (50). The CSFV strain Alfort was obtained from the Institut für Virologie, Hanover, Germany. BVDV-1 CP strain PE515 was obtained from J. M. Aynaud (INRA, Thiverval, France), and BVDV-1 NCP strain Marloie, BVDV-1 NCP strain L2565, and BVDV-2 CP strain 3435 are field isolates obtained from the Veterinary and Agrochemical Research Center (Ukkel, Belgium). Border disease virus (BDV) NCP strain Aveyron was obtained from E. Thiry, University of Liège, Liège,

Belgium. Human hepatoma cells (Huh 7) containing subgenomic HCV replicons I$_{389}$luc-ubi-neo/NS3-3′/5.1 (Huh 5-2) were kindly provided by R. Bartenschlager (University of Heidelberg, Heidelberg, Germany) and were used to assess activity against HCV. Huh 5-2 cells were grown in Dulbecco's modified Eagle's medium (DMEM; Gibco) supplemented with 10% heat-inactivated FBS (Integro), 1× nonessential amino acids (Gibco), 100 IU/ml penicillin (Gibco), 100 μg/ml streptomycin (Gibco), and 250 μg/ml Geneticin (Gibco). GB virus strain B (GBV-B) was propagated in primary tamarin (*Saguinus mystax*) hepatocytes (27). Yellow fever virus (YFV; strain 17D) was the vaccine strain Stamaril from Aventis Pasteur S.A.

Anti-BVDV assay for CP strains (MTS). MDBK cells were seeded at a density of 5 × 10^3 cells per well in 96-well cell culture plates (confluence, 10 to 15%) in MEM-FBS. Following 24 h of incubation at 37°C and 5% CO$_2$, medium was removed and fivefold serial dilutions of the test compounds were added in a total volume of 100 μl, after which the CP BVDV inoculum (multiplicity of infection = 2) was added to each well. This inoculum resulted in a greater than 90% destruction of the cell monolayer after 3 days of incubation at 37°C. Uninfected cells and cells receiving virus without compound were included in each assay plate. After 5 days, medium was removed, and 90 μl of MEM-FBS supplemented with 10 μl of 3-(4,5-dimethylthiazol-2-yl)-5-(3-carboxymethoxyphenyl)-2-(4-sulfophenyl)-2*H*-tetrazolium/phenazinemethosulfate (MTS/PMS) solution (Promega, Leiden, The Netherlands) was added to each well. Following a 2-h incubation period at 37°C, the optical density of each well was read at 490 nm in a microplate reader (signal to noise ratio = 5). The percent CPE was calculated as follows: %CPE = [(OD$_{treated}$)$_{BVDV}$ − (OD$_{control}$)$_{BVDV}$]/{[(OD$_{control}$)$_{mock}$] − (OD$_{control}$)$_{BVDV}$}, in which (OD$_{treated}$)$_{BVDV}$ is the OD$_{490}$ of cells infected with BVDV and treated with a certain dilution of compound, (OD$_{control}$)$_{BVDV}$ is the OD$_{490}$ of cells infected with BVDV and left untreated, and (OD$_{control}$)$_{mock}$ is the OD$_{490}$ of cells mock infected and left untreated. The 50% effective concentration (EC$_{50}$) was defined as the concentration of compound that offered 50% protection of the cells against virus-induced cytopathic effect (CPE) and was calculated using logarithmic interpolation.

Anti-BVDV assay for NCP strains (enzyme-linked immunosorbent assay). The antiviral assay was performed as described above, but evaluation of viral replication was done by means of an enzyme-linked immunosorbent assay method. At 3 days postinfection, cell culture fluid was removed and plates were washed once with phosphate-buffered saline (PBS) and dried for 1 h at 37°C. Next, plates were frozen for 20 min at −80°C, fixed for 10 min in 4% formaldehyde, and washed twice with PBS, after which they were incubated with an anti-BVDV polyclonal serum (diluted 200-fold in 5% horse serum [Gibco], 500 mM NaCl, 1% Tween 80) for 90 min at 37°C. Plates were then washed three times with wash buffer (150 mM NaCl, 1% Tween 80), and a 500-fold dilution of anti-bovine-coupled peroxidase antibody (Sigma) in dilution buffer was added for 1 h at 37°C. Following three wash steps, plates were incubated with detection buffer (4 mg 3-amino-9-ethylcarbazole dissolved in 1 ml *N,N*-dimethylformamide and 14 ml of 0.1 M acetate buffer [pH 5.2] containing 150 μl of 3% H$_2$O$_2$) for 15 min until a dark red color appeared. EC$_{50}$ values were calculated using the method of Reed-Muench (41).

Anti-CSFV and BDV assays. Antiviral assays with CSFV and BDV were performed in a similar manner as the antiviral assay with the BVDV NCP strains. For CSFV, PK15 cells (ATCC CCL-33) were used. Infected cells were stained with a polyclonal anti-CSFV serum conjugated with biotin, and streptavidin-conjugated horseradish peroxidase was used as secondary antibody. For BDV, MDBK cells were used. Infected cells were stained using an anti-BDV polyclonal serum (bovine origin) as primary antibody and an anti-bovine-coupled peroxidase antibody as secondary antibody. Plates were stained and read as described above.

Anti-GBV-B assay. Antiviral assays of GBV-B were essentially performed as described previously (27).

Anti-HCV assay. Huh 5-2 cells (3; Paeshuyse et al., unpublished) were seeded at a density of 5 × 10^3 cells per well (confluence, 10 to 15%) in a white view 96-well plate (Perkin-Elmer, Boston, Mass.) in complete DMEM supplemented with 250 μg/ml G418. Following a 24-h incubation at 37°C and 5% CO$_2$, medium was removed and threefold serial dilutions of compound in complete DMEM were added in a total volume of 100 μl. After an incubation period of 4 days at 37°C, cell culture fluid was removed and luciferase activity was assessed by means of the Steady-Glo luciferase assay system (Promega) and a Luminoskan Ascent (Thermo, Vantaa, Finland). The EC$_{50}$ was defined as the concentration of compound that reduced the luciferase signal with 50% and was calculated as described for BVDV.

Cytostatic assay. MDBK or Huh 5-2 cells were seeded at a density of 5 × 10^3 cells per well in a 96-well plate (confluence 10 to 15%) in MEM-FBS; 24 h later, serial dilutions of the test compounds were added. Cells were allowed to proliferate for 3 days at 37°C, after which the cell number was determined by means of the MTS/PMS (Promega) method (signal to noise ratio = 5). The percent cell
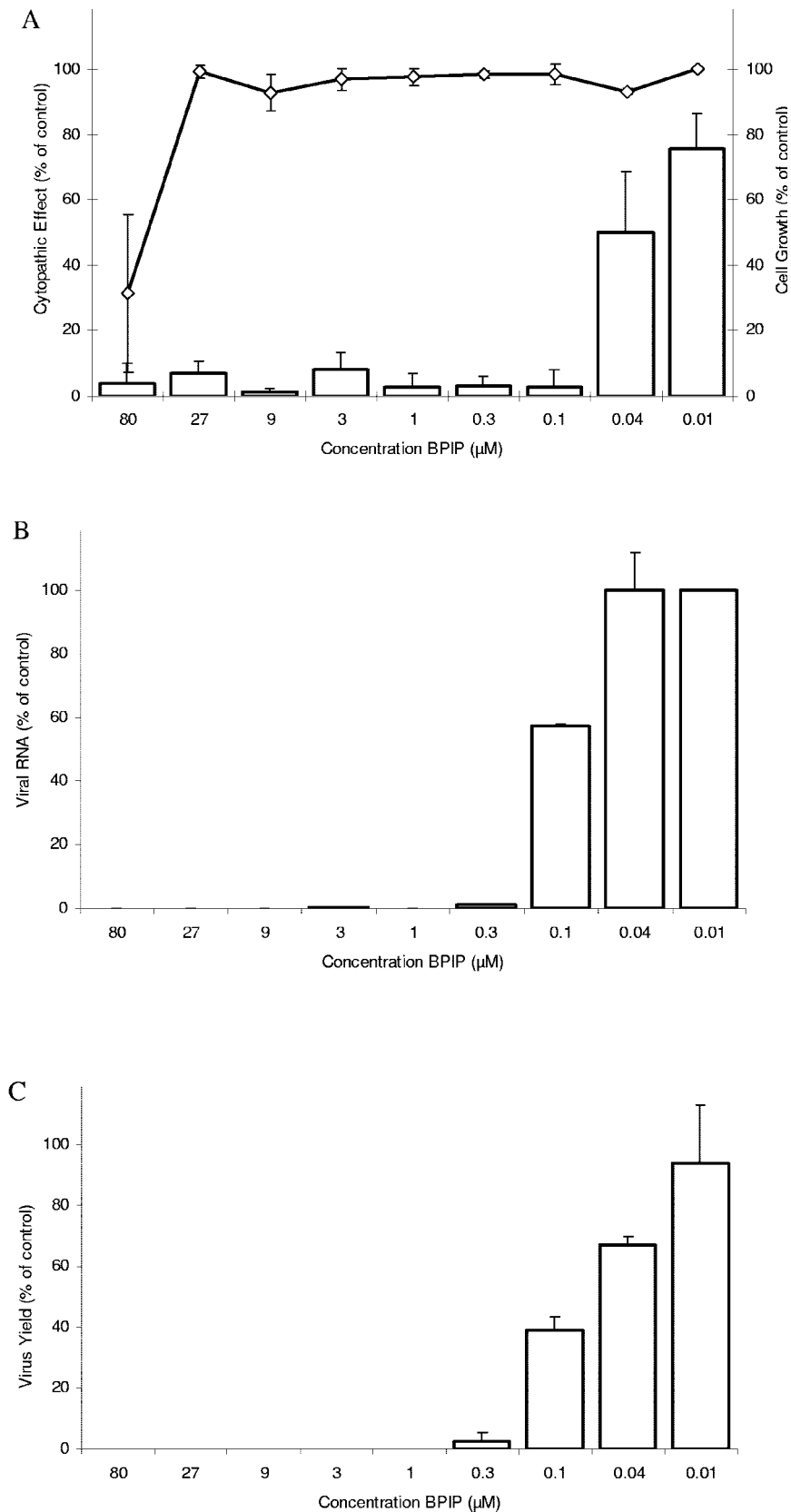
FIG. 1. (A) Effect of BPIP on BVDV (strain NADL)-induced CPE formation in MDBK cells (bars) and on the proliferation of exponentially growing MDBK cells (diamonds). BPIP caused, at concentrations above 0.3 μM, complete inhibition of BVDV-induced CPE, as assessed microscopically (although not evident from the MTS assay at these concentrations). (B) Inhibitory effect of BPIP on release of extracellular viral RNA. (C) Inhibitory effect of BPIP on infectious virus yield.

growth was calculated as $(OD_{treated})/(OD_{control})$, in which $(OD_{treated})$ is the OD_{490} of cells treated with a certain dilution of compound and $(OD_{control})$ is the OD_{490} of cells left untreated. The 50% cytostatic concentration (CC_{50}) was defined as the concentration that inhibited the proliferation of exponentially growing cells by 50% and was calculated using logarithmic interpolation.

Time of drug addition studies. MDBK cells (6.5×10^5 cells/well; confluence, 10 to 15%) were seeded in a six-well culture plate (Asahi Technoglass Corporation, Tokyo, Japan). Cultures were inoculated with BVDV (strain NADL; multiplicity of infection = 2). The inoculum was removed following a 1-h incubation period, and cells were washed three times with prewarmed PBS. To obtain precise information on the replication kinetics of BVDV in untreated cultures, supernatant and cells were harvested every 2 h and samples were stored at −80°C until further use. In a parallel set of cultures, the test compounds (at 15 μM) were added at different time points after infection. Cultures were further incubated until 24 h postinfection, at which time cell culture supernatant was collected and stored at −80°C until further use.

Virus yield assay. MDBK cells were seeded at a density of 5×10^3 cells per well of a 96-well plate (confluence, 10 to 15%) in MEM-FBS and were, 24 h later, infected with 10-fold serial dilutions of culture supernatant. After 4 days, medium was removed and cultures were fixed with 70% ethanol, stained with Giemsa solution, washed, and air dried. Virus-induced CPE was recorded microscopically, and the viral titer was quantified according to the method of Reed and Muench (41). Viral titers were expressed as cell culture 50% infectious dose (per milliliter).

Isolation of BPIP-resistant BVDV. BPIP-resistant (BPIP^r) virus was generated by culturing wild-type BVDV in MDBK cells in the presence of increasing concentrations of the compound. After 3 days of incubation, cultures were freeze-thawed. Lysates of infected and treated cultures that exhibited a cytopathic effect under drug selection were used to infect new cell monolayers. These were further incubated in the presence of higher concentration of the compound. The procedure was repeated (12 passages) until drug-resistant virus was selected. The putative drug-resistant viruses were plaque purified twice in the presence of 10 μg/ml of BPIP.

Introduction of the F224S mutation in a BVDV infectious clone. Introduction of the F224S mutation (TTC to TCC) in the NS5B gene in pNADLp15a and generation of infectious viral particles was carried out essentially as described previously (50).

RNA isolation. Viral RNA was isolated from cell culture supernatant using the QIAamp viral RNA minikit (QIAGEN, Venlo, The Netherlands). Total cellular RNA was isolated from cells using the RNeasy minikit (QIAGEN).

RT-qPCR. A 50-μl RT-quantitative PCR (qPCR) reaction contained TaqMan EZ buffer (50 mmol/liter Bicine, 115 mmol/liter potassium acetate, 0.01 mmol/liter EDTA, 60 nmol/liter 6-carboxy-X-rhodamine, and 8% glycerol, pH 8.2; Applied Biosystems, Nieuwerkerk, The Netherlands), 200 μmol/liter dATP, 200 μmol/liter dGTP, 200 μmol/liter dCTP, 500 μmol/liter dUTP, 300 nmol/liter forward primer (5′-TGA GCT GTC TGA AAT GGT CGA TT-3′), 300 nmol/liter reverse primer (5′-AGA AAT ACT GGG TCA TCT GAT GCA A-3′), 300 nmol/liter TaqMan probe (6-carboxyfluorescein-CGA AGC AGG TTA CCA AGG AGG CTG TTA GGA-6-carboxytetramethylrhodamine), 3 mmol/liter manganese acetate, 0.5 U AmpErase uracil-*N*-glycosylase (UNG), 7.5 U r*Tth* DNA polymerase, and template BVDV RNA. Following initial activation by UNG at 50°C for 2 min, the RT step was performed at 60°C for 30 min, followed by inactivation of UNG at 95°C for 5 min. Subsequent PCR amplification consisted of 40 cycles of denaturation at 94°C for 20 s and annealing and extension at 62°C for 1 min in an ABI 7000 sequence detector. All samples were analyzed in three replicate reactions.

Sequencing. PCR fragments that cover the entire BVDV genome were generated and analyzed using the cycle-sequencing method (ABI Prism BigDye Terminator Cycle Sequencing Ready Reaction kit). Both DNA strands were sequenced. Sequence data were obtained using an ABI 373 Automated Sequence Analyzer (Applied Biosystems), and sequences were analyzed using the Vector NTI software package (Invitrogen, Merelbeke, Belgium).

RC assay. The RC assay was essentially similar, as published by Sun and colleagues (47). In brief, BVDV-infected MDBK cells were suspended in ice-cold hypotonic buffer A (10 mM Tris-HCl [pH 7.4], 1.5 mM $MgCl_2$) and were incubated for 30 min on ice, after which they were further disrupted by 20 strokes with a Dounce homogenizer. The disrupted cells were pelleted by centrifugation at $1,000 \times g$ for 5 min at 4°C. The supernatant fraction, containing cytoplasmic material and plasma membranes, was concentrated by high-speed centrifugation at $200,000 \times g$ for 30 min at 4°C. The pellet was resuspended in 120 μl of buffer B (10 mM Tris-HCl [pH 8.0], 10 mM NaCl, 15% glycerol) and used for an RNA polymerase assay. Replicase reactions were carried out in a total volume of 50 μl in 50 mM HEPES (pH 8.0), 50 mM potassium acetate, 3 mM $MgCl_2$, 10 mM

dithiothretol, 5 mM creatine phosphate, 25 μg/ml creatine phosphokinase, 1 mM ATP, 0.5 mM GTP, 0.5 mM CTP, 40 μM UTP, 10 μCi of [α-^{33}P]UTP (3,000 mCi/mmol) (Amersham, Uppsala, Sweden), 40 U of RNasin (Promega), and 20 μl of the membrane preparation. Following incubation at 30°C for 1 h, the reactions were stopped by adding sodium dodecyl sulfate up to 1% and extracted twice with phenol-chloroform. The RNA products were precipitated in ethanol and analyzed on a 0.6% denaturing glyoxal-agarose gel. Radioactivity incorporated into virus-specific RNA was quantitated using ImageQuant software for the Storm 820 PhosphorImager (Amersham) and expressed as % replication = (density sample/density of untreated control) × 100.

RNA-dependent RNA polymerase reaction. BVDV (strain NADL) RdRp was expressed and purified as described before (57). The purified BVDV polymerase (100 nM) was mixed with 100 μM GTP (containing 8.3 μM of [^{3}H]GTP; Amersham) and increasing concentrations of inhibitor (0.1 μM, 10 μM, and 96 μM for BPIP or 100 μM for the other inhibitors) in 50 mM HEPES, pH 8.0, 10 mM KCl, 10 mM DTT, 1 mM $MgCl_2$, 2 mM $MnCl_2$, and 0.5% igepal (Sigma). Enzyme mix and inhibitors were preincubated (30 min) in order to favor enzyme-inhibitor interaction before RNA binding in case of competition for the RNA-binding site. Reactions were started by the addition of 100 nM poly(C) (about 500 nucleotides in size) template. Reactions were incubated at 30°C and stopped by the addition of 50 mM EDTA after 1, 5, or 15 min. Samples were transferred onto DE-81 filters, washed with 0.3 M ammonium formate, and dried. Radioactivity bound to the filter was determined by liquid scintillation counting. The assay was also carried out as described above except that the poly(C) template was replaced by either oligo(dT)/poly(A), oligo(G)/poly(C), or an artificial hairpin (this is, an RNA transcript that encompasses nucleotides 1,768 to 2,016 of the sequence with accession number AF305422).

Computational docking. The published X-ray structure of the BVDV RdRp by Protein Data Bank (PDB) entry 1S48 (9) was used in all docking experiments. Selenium atoms in the selenomethionine residues were modified back to S atoms to get methionine residues. Explicit hydrogen atoms were added to the enzyme and inhibitor structures using Reduce (55). The inhibitor BPIP was drawn using Macromodel 5.0 (36). The molecular geometry was optimized in the Amber force field (54) and saved as a PDB file. This file was fed into Gamess for geometry optimization using the AM1 force field (42). The PDB file was then converted to mol2 files using Babel. The position of atom CZ in F224 in the published PDB file 1S48 was used as the center of the docking sphere with a sphere radius of 6.0 Å. Because there is no clear cavity in the neighborhood of F224, the "detect cavity" option was turned off. Default settings were used in Gold for all dockings (22, 23). The structures in the top 50 of the docking scores were retained for visual inspection and analysis. One docked BPIP conformation was retained for further analysis. Criteria to withhold this docked complex were stacking interaction with the F224 phenyl ring, hydrogen bonding, and hydrophobic interactions. Molecular energy optimization of docked complex was carried out using the Amber software. This complex was energy-minimized using the Amber 8.0 software (37). The Amber ff03 force field (11) was used for all polymerase atoms. The BPIP inhibitor parameters and atomic charges were from the general Amber force field by running the Antechamber program (53). The complex was then relaxed by a short energy minimization (500 steps) in the Sander program. The nonbonded cutoff was set to at least 12 Å. Then a further energy minimization of 5,000 steps was performed on the inhibitor and all residues having atoms within a 15 Å distance from an inhibitor atom.

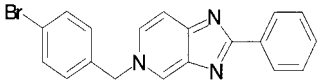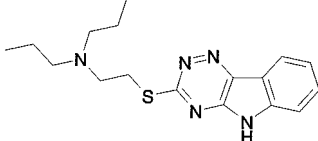**Intracellular metabolism of BPIP.** MDBK cell cultures were incubated for 10 h with 55 μM BPIP. Then cultures were washed three times with PBS. Cells were trypsinized and resuspended in PBS, and equal volumes of cell suspension and ethyl acetate were combined. Samples were vortexed three times for 30 s, and the aqueous phase was snap frozen in an ethanol dry ice mixture. The organic phase was transferred to a new centrifuge tube, and the ethyl acetate was evaporated in a vacuum centrifuge at 40°C for 1 h. Prior to detection, samples were dissolved in 50% methanol. Separation and analysis were carried out using a capillary liquid chromatograph (CapLC; Waters, Milford, MA) connected to a Q-Tof-2 mass spectrometer (Micromass, Manchester, United Kingdom). Samples were separated on a reverse-phase column (XTerra column 0.32 × 50 mm, Waters) with a gradient of 0.1% formic acid and acetonitrile at a flow rate of 5 μl/min. This setup has a dynamic range of over 3 orders of magnitude, allowing the detection of the presence of less than 0.1% impurities and metabolites.

RESULTS

Antiviral activity of BPIP. Following optimization of a lead compound, BPIP (Table 1) was identified in a multicycle

TABLE 1. Effect of BPIP and VP32947 on the replication of various *Flaviviridae*

Compound	Structure	EC_{50} (μM)[a]			
		BVDV	YFV	HCV	GBV-B
BPIP		0.04 ± 0.01	>50	>50	17.6 ± 0.8
VP32947		0.03 ± 0.01	>50	>50	

[a] EC_{50} of BPIP and VP32947 for inhibition of BVDV (strain NADL) replication in MDBK cells, YFV (strain 17D) replication in Vero cells, HCV subgenomic replicon (genotype 1b) replication in Huh 5-2 cells, and GBV-B replication in primary tamarin hepatocytes. Data are given as mean values $\pm$ standard deviations from at least two independent experiments.

growth assay in MDBK cells as a highly selective inhibitor of BVDV (strain NADL) replication. The EC_{50} as assessed by monitoring CPE reduction by the MTS method was 0.04 ± 0.01 μM. The compound inhibited virus-induced CPE formation in a dose-dependent way (Fig. 1A). To confirm the anti-BVDV activity of BPIP, the effect of the compound on viral RNA synthesis (Fig. 1B) and on infectious viral yield was determined (Fig. 1C). Overall, the pattern of inhibition of viral RNA synthesis and infectious virus yield were very similar (Fig. 1A, B, and C). The EC_{50} for inhibition of viral RNA production in culture supernatant was 0.12 ± 0.02 μM and for inhibition of infectious virus yield was 0.074 ± 0.003 μM. BPIP also inhibited the replication of four other BVDV-1 strains (of which two were NCP strains and two were CP strains), as well as a BVDV-2 CP strain (Table 2). Moreover, the compound inhibited the replication of the CSFV (strain Alfort) and the BDV (strain Aveyron) (Table 2). The activity of BPIP against the latter viruses was assessed by an immunohistochemical method. The resulting EC_{50} values obtained were three- to eightfold higher than the EC_{50} value obtained by means of the other methods (the reason for which is unclear but may be related to overstaining and thus underestimating the antiviral activity). BPIP exhibited an only modest inhibitory effect on GBV-B replication ($EC_{50} = 17.5 \pm 0.7$ μM) and had no inhibitory effect on the replication of hepatitis C virus subgenomic replicons (genotype 1b) or the yellow fever virus (vaccine strain 17D), a flavivirus (Table 1). The replication of unrelated RNA or DNA viruses (such as respiratory syncytial virus, coxsackievirus B3, herpes sim-

plex virus [types 1 and 2], and human immunodeficiency virus type 1) was not inhibited by BPIP (data not shown). BPIP is relatively noncytotoxic: the concentration that reduced the proliferation of exponentially growing MDBK cells by 50% (CC_{50}) was 80 ± 11 μM. (Fig. 1A). This is almost equal to the solubility limit of 96 μM (data not shown). Hence, a selectivity index (against BVDV strain NADL) or the ratio of CC_{50}/EC_{50} of about 2,000 was calculated.

Intracellular metabolism of BPIP. To study whether intracellular metabolites of BPIP are formed, that may represent, rather than BPIP itself, the active antiviral component, the intracellular metabolism of BPIP in MDBK cells was analyzed. Cellular extracts from MDBK cells that had been treated for 10 h with 55 μM BPIP were analyzed by reverse-phase high-performance liquid chromatography connected to a mass spectrometer. Only intact BPIP, but no metabolites or degradation products, could be detected.

Time-of-(drug) addition studies. To understand at what time during the viral replication cycle BPIP interferes with viral replication, detailed time-of-(drug) addition experiments were carried out. The kinetics of one replication cycle of BVDV was first determined by means of both RT-qPCR and viral yield assay. It was ascertained that a linear correlation exists between extracellular viral RNA and infectious virus yield ($R^2 = 0.99$). In untreated cells, release of viral RNA (Fig. 2A) and infectious viral particles (Fig. 2A) into the supernatant was first detected between 12 and 14 h postinfection; hence, under our experimental conditions, a single cycle of BVDV growth takes an average of 13 h

TABLE 2. Effect of BPIP on pestivirus replication

Virus	Strain	Biotype	EC_{50} (μM)[a]			
			ELISA	MTS	RT-qPCR	Virus yield
BVDV-1	L2565	NCP	0.6 ± 0.2			
	Marloie	NCP	0.5 ± 0.2			
	PE515	CP	0.1 ± 0.2			
	NADL	CP	0.33 ± 0.03	0.04 ± 0.01[b]	0.12 ± 0.02	0.074 ± 0.003
BVDV-2	3435	CP	0.2 ± 0.1			
CSFV	Alfort		2 ± 1			
BDV	Aveyron		1.7 ± 0.5			

[a] Data are given as mean values $\pm$ standard deviations from three independent experiments.
[b] EC_{50} of VP32947 for the inhibition of BVDV NADL replication in MDBK cells (as assessed in parallel by means of the MTS assay) was 0.03 ± 0.01 μM.
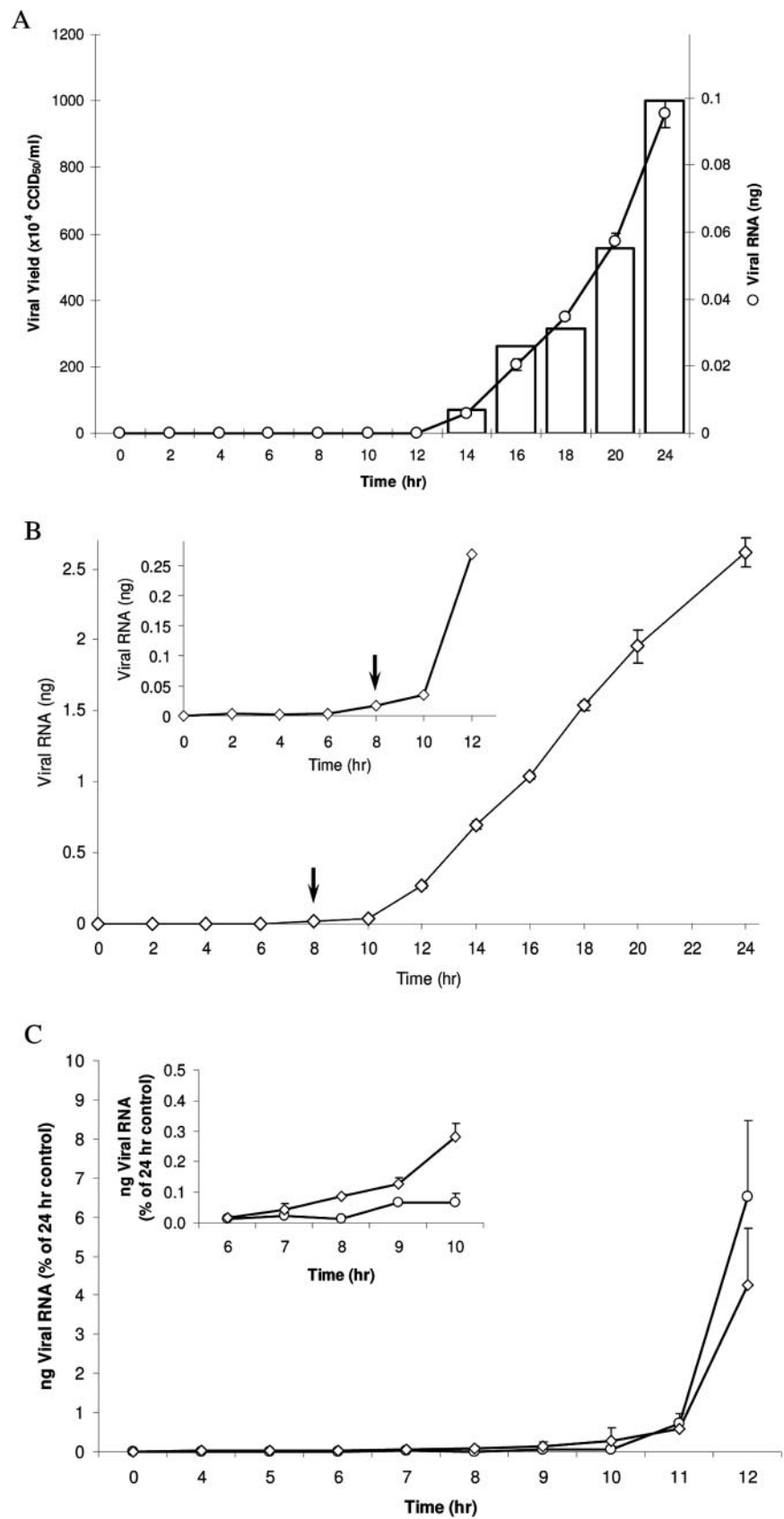
A

B

C

TABLE 3. Susceptibility of wild-type and BPIP[r] BVDV to BPIP, VP32947, and 2′-*C*-methyladenosine

Virus	EC$_{50}$ (μM)[a]		
	BPIP	VP32947	2′-*C*-methyladenosine
BVDV (NADL)	0.051 ± 0.005	0.025 ± 0.003	0.4 ± 0.1
BVDV (selected BPIP[r])	55 ± 5	8 ± 2	0.35 ± 0.02
BVDV (recombinant BPIP[r])	49 ± 14	9 ± 3	0.37 ± 0.06

[a] Data are given as mean values ± standard deviations from three independent experiments.

(Fig. 2A). As of 6 to 8 h postinfection, a gradual increase of intracellular viral RNA was noted (Fig. 2B). This rise must coincide with the formation of functional RCs which produce viral RNA. When BPIP was added during the first 8 h postinfection, it resulted in the complete inhibition of extracellular (Fig. 2C) and intracellular (Fig. 2C) viral RNA yield, as detected at 24 h postinfection. A gradual loss in the antiviral efficacy of BPIP was noted when the compound was first added at a time point later than 8 h postinfection.

Isolation and characterization of drug-resistant viruses. BPIP[r] virus was selected by propagating BVDV (strain NADL) for 12 passages in increasing concentrations (from 0.2 to 27 μM) of the drug. The resulting drug-resistant virus pool was plaque purified twice in the presence of a 27 μM concentration of the compound. The plaque-purified BPIP[r] virus proved to be at least a 300-fold less susceptible to the inhibitory effect of BPIP than the parent wild-type strain (Table 3). The resistant virus replicated about as efficiently as the parent wild-type virus. VP32947, which was included as a reference drug, showed cross-resistance with BPIP. By contrast, 2′-*C*-methyladenosine, a nucleoside analogue inhibitor of HCV (8, 15) that we also found to be active against BVDV, was equally active against the wild type as it was against the BPIP-resistant virus (Table 3).

Molecular characterization of BPIP-resistant virus. Since the BPIP[r] virus proved to be cross-resistant with VP32947, the region in which the mutation was found that resulted in resistance against VP32947 was sequenced. By comparing the sequences of this region obtained from six independently isolated BPIP[r] clones to the parent wild-type strain (GenBank accession no. AJ781045), we identified a T-to-C transition at position 10,863 in the viral RNA. This point mutation resulted in an amino acid change of phenylalanine (F) to serine (S) at amino acid residue 224 in the mature NS5B protein. Subsequently, the remaining part of the nonstructural (NS) region of the genome of BPIP[r] clones was sequenced. No other mutations were detected throughout the NS region of the genome of the drug-resistant virus.

To confirm that the F224S change in NS5B alone was responsible for the BPIP[r] phenotype, the mutation was introduced in the infectious clone pNADLp15a of the wild-type virus. RNA transcripts derived from plasmid pNADLp15a/DR were transfected into MDBK cells, and the resulting recombinant BPIP[r] virus was isolated. Sequence analysis confirmed that this virus indeed carried the F224S mutation. Akin to the original selected BPIP[r] virus, the recombinant BPIP[r] virus was resistant to the inhibitory effects of BPIP and VP32947 but remained sensitive to the antiviral activity of 2′-*C*-methyladenosine (Table 3).

In vitro RdRp assay. BPIP, VP32947, and the nucleotide analogues 3′-dGTP, 2′-*C*-Me-GTP, and 2′-*O*-Me-GTP (included as positive controls) were studied for their effects on the polymerase activity of highly purified BVDV RdRp by using poly(C) as a template. BPIP had no, and VP32947 only a minor, effect on the activity of the viral polymerase (Fig. 3). The 50% inhibitory concentrations for BVDV polymerase activity were <1 μM for 3′-dGTP, ∼1 μM for 2′-*C*-Me-GTP, and between 5 and 10 μM for 2′-*O*-Me-GTP. The effect of BPIP on the purified BVDV RdRp was further assessed using various RNA templates [oligo(dT)/poly(A), oligo(G)/poly(C), and an artificial hairpin]. No significant inhibition by BPIP of the activity of the viral polymerase was noted when these other templates were used (data not shown).

Viral replicase complex assay. Because BPIP did not inhibit the activity of the purified BVDV RdRp, the effect of the compound on viral RCs, isolated from MDBK cells that had been infected with the wild-type virus, was studied. BPIP almost completely inhibited the activity of the BVDV RCs over a concentration range of 0.5 to 10 μM (Fig. 4A, B). In contrast, BPIP had only a weak inhibitory effect on the activity (maximum 50% at concentrations as high as 10 μM) of RCs isolated from MDBK cells that had been infected with the laboratory-selected BPIP[r] virus (Fig. 4A, B).

Computational docking of BPIP in the BVDV RdRp crystal structure. Molecular modeling revealed that F224 is located at the tip of the finger domain of the BVDV polymerase. Docking of BPIP to the BVDV RdRp and performing a Ligplot/HBPlus analysis (34, 52) (Fig. 5C) on the docking complex revealed possible interactions between the polymerase and BPIP. One possible interaction was in agreement with our hypothesis that this inhibitor should bind close to the F224 residue. Through this analysis (Fig. 5A, C), the following interactions were suggested: (i) a stacking interaction between the imidazo[4,5-c]pyridine ring system of BPIP and F224, the average distance between both aromatic systems is about 3.5 Å, (ii) hydrophobic contacts of the inhibitor with A221, A222, and F224, and (iii) a hydrogen bond between N3 of the imidazole ring in BPIP with the backbone oxygen of residue F224 (distance, 3.27 Å).

FIG. 2. Yields of extracellular viral RNA (circles), infectious virus (bars), or intracellular viral RNA (diamonds) during a single replication cycle of BVDV strain NADL in MDBK cells. Viral RNA levels were monitored at various times postinfection by RT-qPCR. (A) Extracellular viral RNA and infectious virus yields during a time course of 24 h. (B) Intracellular viral RNA yields over a time course of 24 h (the inset presents the viral RNA levels during the period from 0 to 12 h on a more detailed scale). CCID$_{50}$, cell culture 50% infectious dose. (C) Effect of time-of-(drug) addition on the antiviral activity of BPIP. Extracellular and intracellular viral RNA was monitored by RT-qPCR at 24 h postinfection (in cells treated with BPIP [at 15 μM], starting at different times postinfection) and compared with untreated infected cells (the inset presents the viral RNA levels during the period 6 to 10 h on a more detailed scale). Values are expressed as percentages of viral RNA of untreated infected cells.
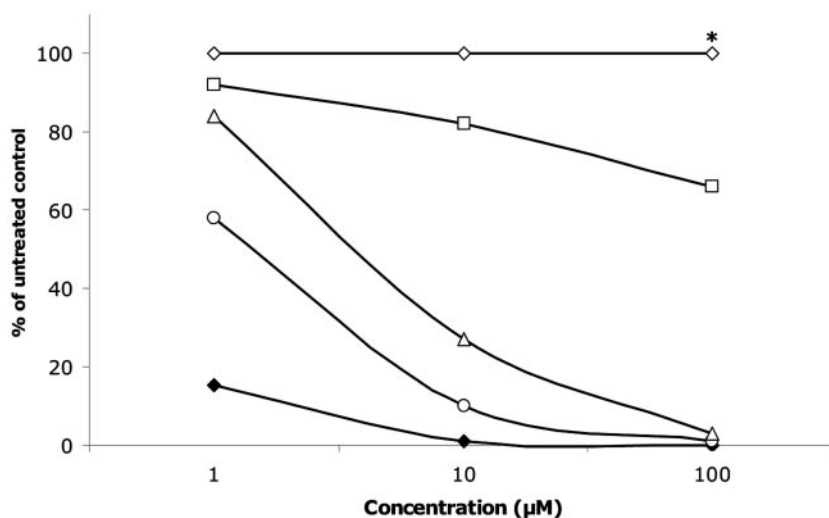
FIG. 3. Effect of BPIP (open diamonds), VP32947 (open squares), 3′-dGTP (open triangles), 2′-C-Me-GTP (open circles), and 2′-O-Me-GTP (filled diamonds) on the activity of purified BVDV RdRp using poly(C) as a template and incubated for 5 min. Data are from a typical experiment and are expressed as the percentage of untreated control. Similar data were obtained using other templates. BPIP was tested at the highest concentration of 96 μM (*).

No specific interaction of the inhibitor's Br atom with the enzyme emerged from this analysis.

DISCUSSION

A small molecule (BPIP) was identified (following lead optimization) as a highly selective and potent in vitro inhibitor of the replication of pestiviruses. The compound proved highly active against both cytopathic and noncytopathic biotypes of BVDV-1 and BVDV-2 as well as against other members of the genus *Pestivirus*, i.e., classical swine fever virus and border disease virus.

BPIP was inactive against the hepacivirus HCV (as assessed in the HCV genotype 1b subgenomic replicon system) and against the flavivirus YFV strain 17D but exhibited moderate activity against GBV-B. However, when the entire series of compounds that were synthesized during lead optimization for anti-BVDV activity were evaluated against HCV, a few molecules were found to inhibit the replication of this virus in the replicon system. Molecules in this series of imidazopyridines could be classified in three groups: (i) compounds solely active against BVDV, (ii) compounds active against both BVDV and HCV, and (iii) compounds active only against HCV. Studies on the structure-activity relationship of the anti-BVDV and anti-HCV series will be reported elsewhere. These data demonstrate for the first time that distinct changes to a class of small molecule inhibitors of pestivirus replication may result in molecules with antihepacivirus activity, despite the fact that the most potent antipestivirus molecules in this series are devoid of anti-HCV activity.

We then further focused on the mechanism of anti-BVDV activity of BPIP. Detailed time-of-(drug) addition studies revealed that the time point at which BPIP exerts its activity coincided with the onset of viral RNA synthesis at about 8 h postinfection. Addition of compound at a time point before the onset of intracellular viral RNA synthesis led to the complete inhibition of viral RNA production, whereas addition at later time points resulted in a gradual loss of antiviral activity. These data suggest that BPIP interferes with the formation or function of the replication complex of the virus. When the genotype of in vitro-generated BPIPr virus was determined, a phenylalanine (F)-to-serine (S) mutation was detected (in six out of six sequenced clones) at position 224 (F224S) of the NS5B, the gene that encodes the viral RNA-dependent RNA polymerase. No other mutations were detected throughout the NS region of the drug-resistant virus.

Introduction of the F224S mutation in a full-length wild-type infectious clone of BVDV (strain NADL) again resulted in the drug-resistant phenotype. This confirms that the F224S mutation indeed is responsible for the resistant phenotype. The phenylalanine residue at position 224 of the RdRp is almost strictly conserved within the genus pestivirus. Only BVDV type 2 carries a tyrosine at this position. BVDV-2 is roughly equally susceptible to BPIP as BVDV-1 and the other pestiviruses. This may not be surprising, as tyrosine and phenylalanine (but not serine) share similar aromatic properties. Interestingly, the antipestivirus compound VP32947, a molecule that has a chemical structure that is very different from that of BPIP, induced the same mutation. In line with this observation, VP32947 proved cross-resistant with BPIP. In contrast, the nucleoside analogue 2′-C-methyladenosine was equally effective against both wild-type and BPIP-resistant virus.

Although the drug-induced mutation in the viral RdRp strongly suggests interference with the viral polymerase activity, we were unable to detect inhibition of the highly purified enzyme with BPIP (or with VP32947), even at relatively high concentrations. The fact that two very different compounds induce the same mutation suggests that this amino acid (F224) and its environment play a crucial role in the normal functioning of the BVDV RdRp. The viral polymerase assay was validated by demonstrating that 2′-C-Me-GTP (the 5′-triphosphate metabolite of 2′-C-methyl-guanosine, an analogue of
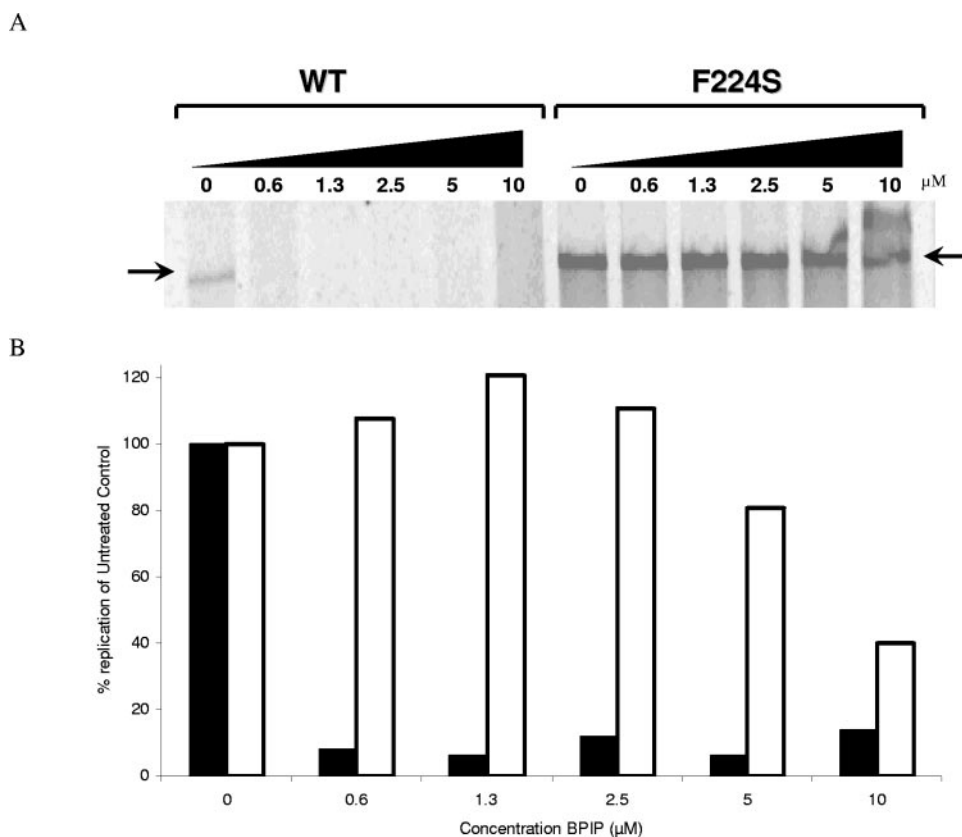
FIG. 4. Effect of BPIP on the activity of replication complexes isolated at 14 h postinfection from MDBK cells that had been infected with the wild type (WT) (strain NADL) or with the selected BPIP[r] BVDV strain. (A) Reaction product of the RC assay was separated on a 0.6% agarose-glyoxal denaturing gel. Replication complexes for this assay were isolated from MDBK cells infected either with WT virus or with the selected BPIP[r] BVDV strain. The arrow indicates the position at which full-length BVDV RNA migrates (confirmed by using molecular weight markers and RNase treatment). (B) Densiometric analysis of the autoradiograph depicted in panel A. Black bars represent the activity of WT (strain NADL) RCs, and open bars represent the activity of RCs from cells infected with selected BPIP[r] virus. % replication = (density sample/density of untreated control) × 100.

2′-C-methyl-adenosine) and related molecules inhibited the BVDV RdRp activity. The lack of activity of VP32947 against BVDV polymerase we observed is consistent with results obtained by King and coworkers (24). However, within the cell, BVDV NS5B functions in the context of membrane-bound RCs that consist of several virus-encoded proteins, host proteins, and various forms of viral RNA (47, 49). We therefore evaluated the effect of BPIP on RCs isolated from MDBK cells that had been infected either with wild-type virus or with the mutant F224S virus. BPIP effectively inhibited the function of the wild-type RC but not that of the mutant RC. A possible explanation for the lack of activity of BPIP on the purified polymerase may therefore be that the compound, following its interaction with NS5B, disturbs the formation/stability/function of the replication complex. Although neither we nor King et al. (24) detected inhibition of the activity of the highly purified polymerase of BVDV NS5B by VP32947, Baginski and coworkers did observe inhibition of the viral polymerase by VP32947 (2). It should be noted, however, that low template concentrations were used in their assay and that the 50% inhibitory concentration for the viral polymerase was 35-fold higher (700 nM) than the EC_{50} for inhibition of viral replication (2). These authors also speculated that VP32947 may

disturb an interaction of NS5B within the BVDV replication complex.

The crystal structure of the RNA-dependent RNA polymerase of BVDV was recently reported (9). The BVDV polymerase shares several structural characteristics with the RdRp of HCV (1, 5, 9, 29). The F224S mutation responsible for resistance to BPIP and VP32947 is located in a turn in the finger domain between two beta-sheets of the BVDV RdRp. The corresponding region in the HCV RdRp is believed to be involved in finger flexibility for template/product translocation (26), dimerization of the RdRp in the replication complex, or protein-protein interactions (10, 38), enabling the assembly of an active replication complex.

Computational docking of BPIP to the BVDV RdRp suggested that there were a limited number of interactions between the inhibitor and the polymerase. Hypothetical binding of the inhibitor to the polymerase could result in reduced finger flexibility or impairment of the ability of the polymerase to translocate its template/product during polymerization. Another possibility could be that the 4-bromophenyl moiety influences the entrance of the template RNA in the template-binding channel. It should be mentioned, however, that
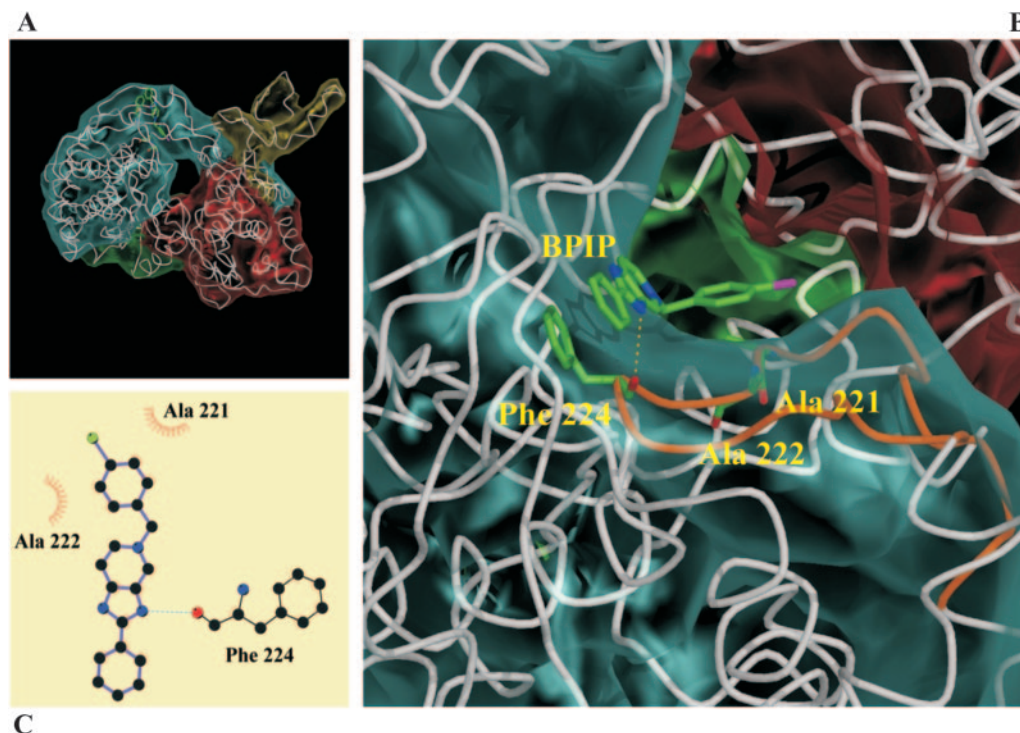
FIG. 5. Modeling of BPIP near the position of F224 in the RNA-dependent RNA polymerase. (A) Overview of the entire structure of the RdRp of BVDV with BPIP docked in the vicinity of F224. (B) Detail of the predicted part of the RdRp surface that possibly interacts with BPIP. The following predicted interactions are shown: (i) a hydrogen bond (presented as a yellow dashed line) and (ii) interacting hydrophobic residues A221, A222, and F224 (highlighted). The loop that contains F224 is colored in cyan (residues 212 to 232). The BVDV polymerase domains are colored yellow (N-terminal domain, residues 1 to 138), blue (fingers, residues 139 to 313 and residues 351 to 410), green (palm, residues 314 to 350 and residues 411 to 500), or red (thumb, residues 501 to 679). Picture was generated using Bobscript, Molscript, and Raster3D (16, 25, 35). (C) Ligplot depicts a schematic diagram of protein-BPIP interactions. The interactions shown are hydrogen bonds (dashed light blue line) and hydrophobic contacts (represented by an arc with spokes radiating toward the ligand atoms they contact, and the contacted atoms are shown with spokes radiating back). Br atom (green circle), carbon atoms (black circles), nitrogen atoms (blue circles), and oxygen atom (red circle) are also illustrated.

computational modeling does not provide hard evidence that the modeled interactions do indeed occur in vivo. If BPIP binds to the RdRp, there is, however, no evidence that this results in an allosteric inhibition of the highly purified polymerase or a reduction of its template-binding capability. Recently, it was shown that the generation of cocrystals with VP32947 was hampered by a dimer interface near the putative binding site of VP32947 in the BVDV RdRp crystal (9). The authors suggested that this dimer could play a significant role in the replication complex. Furthermore, it was suggested that the top of the fingers domain may be a protein-binding site important for interaction with other proteins of the replicase complex. BPIP could possibly prevent the interactions between different proteins of the replication complex. It will now be important to study whether the BPIP analogues that exhibit anti-HCV activity result in drug-resistant mutations at a comparable/homologous position in the HCV RdRp.

In conclusion, we report here on a highly potent and selective inhibitor of the replication of pestiviruses. Structural analogues of this molecule also exhibit anti-HCV activity. It is intriguing that this compound, although very different in chemical structure, appears to possess a similar mechanism of action as VP32947 (2), suggesting that the site of the polymerase with which these two compounds interact may be crucial for the functioning of the polymerase and the viral replication com-

plex. The present study contributes to the understanding on how the polymerases of *Flaviviridae* can be targeted by specific inhibitors.

REFERENCES

1. **Ago, H., T. Adachi, A. Yoshida, M. Yamamoto, N. Habuka, K. Yatsunami, and M. Miyano.** 1999. Crystal structure of the RNA-dependent RNA polymerase of hepatitis C virus. Struct. Fold. Des. **7:**1417–1426.
2. **Baginski, S. G., D. C. Pevear, M. Seipel, S. C. Sun, C. A. Benetatos, S. K. Chunduru, C. M. Rice, and M. S. Collett.** 2000. Mechanism of action of a pestivirus antiviral compound. Proc. Natl. Acad. Sci. USA **97:**7981–7986.

3. **Bartenschlager, R., and V. Lohmann.** 2001. Novel cell culture systems for the hepatitis C virus. Antivir. Res. **52:**1–17.

4. **Branza-Nichita, N., D. Durantel, S. Carrouée-Durantel, R. A. Dwek, and N. Zitzmann.** 2001. Antiviral effect of N-butyldeoxynojirimycin against bovine viral diarrhea virus correlates with misfolding of E2 envelope proteins and impairment of their association into E1-E2 heterodimers. J. Virol. **75:**3527–3536.

5. **Bressanelli, S., L. Tomei, F. A. Rey, and R. De Francesco.** 2002. Structural analysis of the hepatitis C virus RNA polymerase in complex with ribonucleotides. J. Virol. **76:**3482–3492.

6. **Buckwold, V. E., B. E. Beer, and R. O. Donis.** 2004. Bovine viral diarrhea virus as a surrogate model of hepatitis C virus for the evaluation of antiviral agents. Antivir. Res. **60:**1–15.

7. **Bukhtiyarova, M., C. J. Rizzo, C. A. Kettner, B. D. Korant, H. T. Scarnati, and R. W. King.** 2001. Inhibition of the bovine viral diarrhoea virus NS3 serine protease by a boron-modified peptidyl mimetic of its natural substrate. Antivir. Chem. Chemother. **12:**367–373.

8. **Carroll, S. S., J. E. Tomassini, M. Bosserman, K. Getty, M. W. Stahlhut, A. B. Eldrup, B. Bhat, D. Hall, A. L. Simcoe, R. LaFemina, C. A. Rutkowski, B. Wolanski, Z. Yang, G. Migliaccio, R. De Francesco, L. C. Kuo, M. MacCoss, and D. B. Olsen.** 2003. Inhibition of hepatitis C virus RNA replication by 2′-modified nucleoside analogs. J. Biol. Chem. **278:**11979–11984.

9. **Choi, K. H., J. M. Groarke, D. C. Young, R. J. Kuhn, J. L. Smith, D. C. Pevear, and M. G. Rossmann.** 2004. The structure of the RNA-dependent RNA polymerase from bovine viral diarrhea virus establishes the role of GTP in de novo initiation. Proc. Natl. Acad. Sci. USA **101:**4425–4430.

10. **Dimitrova, M., I. Imbert, M. P. Kieny, and C. Schuster.** 2003. Protein-protein interactions between hepatitis C virus nonstructural proteins. J. Virol. **77:**5401–5414.

11. **Duan, Y., C. Wu, S. Chowdhury, M. Lee, G. Xiong, W. Zhang, R. Yang, P. Cieplak, R. Luo, and T. Lee.** 2003. A point-charge force field for molecular mechanics simulations of proteins. J. Comput. Chem. **24:**1999–2012.

12. **Durantel, D., N. Branza-Nichita, S. Carrouée-Durantel, T. D. Butters, R. A. Dwek, and N. Zitzmann.** 2001. Study of the mechanism of antiviral action of iminosugar derivatives against bovine viral diarrhea virus. J. Virol. **75:**8987–8998.

13. **Durantel, D., S. Carrouée-Durantel, N. Branza-Nichita, R. A. Dwek, and N. Zitzmann.** 2004. Effects of interferon, ribavirin, and iminosugar derivatives on cells persistently infected with noncytopathic bovine viral diarrhea virus. Antimicrob. Agents Chemother. **48:**497–504.

14. **Edwards, S., A. Fukusho, P. C. Lefevre, A. Lipowski, Z. Pejsak, P. Roehe, and J. Westergaard.** 2000. Classical swine fever: the global situation. Vet. Microbiol. **73:**103–119.

15. **Eldrup, A. B., C. R. Allerson, C. F. Bennett, S. Bera, B. Bhat, N. Bhat, M. R. Bosserman, J. Brooks, C. Burlein, S. S. Carroll, P. D. Cook, K. L. Getty, M. MacCoss, D. R. McMasters, D. B. Olsen, T. P. Prakash, M. Prhavc, Q. Song, J. E. Tomassini, and J. Xia.** 2004. Structure-activity relationship of purine ribonucleosides for inhibition of hepatitis C virus RNA-dependent RNA polymerase. J. Med. Chem. **47:**2283–2295.

16. **Esnouf, R.** 1999. Further additions to Molscript 1.4, including reading and contouring of electron-density maps. Acta Crystallogr. **277:**505–524.

17. **Frolov, I., E. Agapov, T.-A. J. Hoffman, B. M. Pragai, M. Lippa, S. Schlesinger, and C. M. Rice.** 1999. Selection of RNA replicons capable of persistent noncytopathic replication in mammalian cells. J. Virol. **73:**3854–3865.

18. **Givens, M. D., C. C. Dykstra, K. V. Brock, D. A. Stringfellow, A. Kumar, C. E. Stephens, H. Goker, and D. W. Boykin.** 2003. Detection of inhibition of bovine viral diarrhea virus by aromatic cationic molecules. Antimicrob. Agents Chemother. **47:**2223–2230.

19. **Givens, M. D., D. A. Stringfellow, C. C. Dykstra, K. P. Riddell, P. K. Galik, E. Sullivan, J. Robl, P. Kasinathan, A. Kumar, and D. W. Boykin.** 2004. Prevention and elimination of bovine viral diarrhea virus infections in fetal fibroblast cells. Antivir. Res. **64:**113–118.

20. **Greiser-Wilke, I., B. Grummer, and V. Moennig.** 2003. Bovine viral diarrhoea eradication and control programmes in Europe. Biologicals **31:**113–118.

21. **Houe, H.** 2003. Economic impact of BVDV infection in dairies. Biologicals **31:**137–143.

22. **Jones, G., P. Willet, and R. Glen.** 1995. Molecular recognition of receptor sites using a genetic algorithm with a description of desolvation. J. Mol. Biol. **245:**43–53.

23. **Jones, G., P. Willet, R. Glen, A. Leach, and R. Taylor.** 1997. Development and validation of a genetic algorithm for flexible docking. J. Mol. Biol. **267:**727–748.

24. **King, R. W., H. T. Scarnati, E. S. Priestley, I. De Lucca, A. Bansal, and J. K. Williams.** 2002. Selection of a thiazole urea-resistant variant of bovine viral diarrhoea virus that maps to the RNA-dependent RNA polymerase. Antivir. Chem. Chemother. **13:**315–323.

25. **Kraulis, P.** 1991. MOLSCRIPT: a program to produce both detailed and schematic plots of protein structures. J. Appl. Crystallogr. **24:**946–950.

26. **Lai, V. C., C. C. Kao, E. Ferrari, J. Park, A. S. Uss, J. Wright-Minogue, Z. Hong, and J. Y. Lau.** 1999. Mutational analysis of bovine viral diarrhea virus RNA-dependent RNA polymerase. J. Virol. **73:**10129–10136.

27. **Lanford, R. E., D. Chavez, B. Guerra, J. Y. Lau, Z. Hong, K. M. Brasky, and B. Beames.** 2001. Ribavirin induces error-prone replication of GB virus B in primary tamarin hepatocytes. J. Virol. **75:**8074–8081.

28. **Lauer, G. M., and B. D. Walker.** 2001. Hepatitis C virus infection. N. Engl. J. Med. **345:**41–52.

29. **Lesburg, C. A., M. B. Cable, E. Ferrari, Z. Hong, A. F. Mannarino, and P. C. Weber.** 1999. Crystal structure of the RNA-dependent RNA polymerase from hepatitis C virus reveals a fully encircled active site. Nat. Struct. Biol. **6:**937–943.

30. **Letellier, C., P. Kerkhofs, G. Wellemans, and E. Vanopdenbosch.** 1999. Detection and genotyping of bovine diarrhea virus by reverse transcription-polymerase chain amplification of the 5′ untranslated region. Vet. Microbiol. **64:**155–167.

31. **Lindenbach, B. D., and C. M. Rice.** 2001. Flaviviridae: the viruses and their replication, p. 991–1041. In D. M. Knipe, P. M. Howley, D. E. Griffin, M. A. Martin, R. A. Lamb, B. Roizman, and S. E. Straus (ed.), Fields virology. Lippincott Williams & Wilkins, Philadelphia, Pa.

32. **Lindenbach, B. D., M. J. Evans, A. J. Syder, B. Wolk, T. L. Tellinghuisen, C. C. Liu, T. Maruyama, R. O. Hynes, D. R. Burton, J. A. McKeating, and C. M. Rice.** 2005. Complete replication of hepatitis C virus in cell culture. Science **309:**623–626.

33. **Lohmann, V., F. Korner, J. Koch, U. Herian, L. Theilmann, and R. Bartenschlager.** 1999. Replication of subgenomic hepatitis C virus RNAs in a hepatoma cell line. Science **285:**110–113.

34. **McDonald, I., and J. Thornston.** 1994. Satisfying Hydrogen bonding potential in proteins. J. Mol. Biol. **238:**777–793.

35. **Merritt, E.** 1997. Raster3D photorealistic molecular graphics. Methods Enzymol. **277:**505–524.

36. **Mohamadi, F., N. Richards, W. Guida, R. Liskamp, M. Lipton, C. Caufield, C. Chang, T. Hendrickson, and W. Still.** 1990. An integrated software system for modeling organic and bioorganic molecules using molecular mechanics. J. Comput. Chem. **11:**440–467.

37. **Pearlman, D., D. Case, J. Caldwell, W. Ross, T. Cheatham, S. DeBolt, D. Ferguson, G. Seibel, and P. Kollman.** 1995. AMBER, a computer program for applying molecular mechanics, normal mode analysis, molecular dynamics and free energy calculations to elucidate the structures and energies of molecules. Comp. Phys. Commun. **91:**1–41.

38. **Piccininni, S., A. Varaklioti, M. Nardelli, B. Dave, K. D. Raney, and J. E. McCarthy.** 2002. Modulation of the hepatitis C virus RNA-dependent RNA polymerase activity by the non-structural (NS) 3 helicase and the NS4B membrane protein. J. Biol. Chem. **277:**45670–45679.

39. **Pietschmann, T., and R. Bartenschlager.** 2001. The hepatitis C virus replicon system and its application to molecular studies. Curr. Opin. Drug Discov. Dev. **4:**657–664.

40. Reference deleted.

41. **Reed, L. J., and A. H. Muench.** 1938. A simple method of estimating fifty percent endpoints. Am. J. Hyg. **27:**493–497.

42. **Schmidt, M., K. Baldridge, J. Boatz, S. Elbert, M. Gordon, J. Jensen, S. Koseki, N. Matsunaga, K. Nguyen, S. Su, T. Windus, M. Dupuis, and J. Montgomery.** 1993. General atomic and molecular electronic structure. Syst. J. Comput. Chem. **14:**1347–1363.

43. Reference deleted.

44. **Stegeman, A., A. Elbers, H. de Smit, H. Moser, J. Smak, and F. Pluimers.** 2000. The 1997–1998 epidemic of classical swine fever in the Netherlands. Vet. Microbiol. **73:**183–196.

45. **Stringfellow, D. A., K. P. Riddell, M. D. Givens, P. K. Galik, E. Sullivan, C. C. Dykstra, J. Robl, and P. Kasinathan.** 2005. Bovine viral diarrhea virus (BVDV) in cell lines used for somatic cell cloning. Theriogenology **63:**1004–1013.

46. **Stuyver, L. J., T. Whitaker, T. R. McBrayer, B. I. Hernandez-Santiago, S. Lostia, P. M. Tharnish, M. Ramesh, C. K. Chu, R. Jordan, J. Shi, S. Rachakonda, K. A. Watanabe, M. J. Otto, and R. F. Schinazi.** 2003. Ribonucleoside analogue that blocks replication of bovine viral diarrhea and hepatitis C viruses in culture. Antimicrob. Agents Chemother. **47:**244–254.

47. **Sun, J. H., J. A. Lemm, D. R. O'Boyle II, J. Racela, R. Colonno, and Gao, M.** 2003. Specific inhibition of bovine viral diarrhea virus replicase. J. Virol. **77:**6753–6760.

48. **Thomson, B. J., and R. G. Finch.** 2005. Hepatitis C virus infection. Clin. Microbiol. Infect. **11:**86–94.

49. **Uchil, P. D., and V. Satchidanandam.** 2003. Architecture of the flaviviral replication complex. Protease, nuclease, and detergents reveal encasement within double-layered membrane compartments. J. Biol. Chem. **278:**24388–24398.

50. **Vassilev, V. B., and R. O. Donis.** 2000. Bovine viral diarrhea virus induced apoptosis correlates with increased intracellular viral RNA accumulation. Virus Res. **69:**95–107.

51. **Wakita, T., T. Pietschmann, T. Kato, T. Date, M. Miyamoto, Z. Zhao, K. Murthy, A. Habermann, H. G. Krausslich, M. Mizokami, R. Bartenschlager, and T. J. Liang.** 2005. Production of infectious hepatitis C virus in tissue culture from a cloned viral genome. Nat. Med. **11:**791–796.

52. **Wallace, A., R. Laskowski, and J. Thornton.** 1995. LIGPLOT: a program to generate schematic diagrams of protein-ligand interactions. Protein Eng. **8:**127–134.

53. **Wang, J., R. Wolf, J. Caldwell, P. Kollman, and D. Case.** 2004. Development and testing of a general amber force field. J. Comput. Chem. **25:**1157–1174.

54. **Weiner, P., P. Kollman, D. Nguyen, and D. Case.** 1986. An all atom force field for simulations of proteins and nucleic acids J. Comput. Chem. **7:**230–252.

55. **Word, M., S. Lovell, J. Richardson, and D. Richardson.** 1999. Asparagine and glutamine: using hydrogen atom contacts in the choice of sidechain amide orientation. J. Mol. Biol. **285:**1733–1745.

56. **Zhong, J., P. Gastaminza, G. Cheng, S. Kapadia, T. Kato, D. R. Burton, S. F. Wieland, S. L. Uprichard, T. Wakita, and F. V. Chisari.** 2005. Robust hepatitis C virus infection in vitro. Proc. Natl. Acad. Sci. USA **102:**9294–9299.

57. **Zhong, W., L. L. Gutshall, and A. M. Del-Vecchio.** 1998. Identification and characterization of an RNA-dependent RNA polymerase activity within the nonstructural protein 5B region of bovine viral diarrhea virus. J. Virol. **72:**9365–9369.

58. **Zitzmann, N., A. S. Mehta, S. Carrouee, T. D. Butters, F. M. Platt, J. McCauley, B. S. Blumberg, R. A. Dwek, and T. M. Block.** 1999. Imino sugars inhibit the formation and secretion of bovine viral diarrhea virus, a pestivirus model of hepatitis C virus: implications for the development of broad spectrum anti-hepatitis virus agents. Proc. Natl. Acad. Sci. USA **96:**11878–11882.